Int. J. Heat Mass Transfer. Vol. 27, No. 11, pp. 2101–2110, 1984
Printed in Great Britain

0017 9310/84 $3.00 + 0.00

Onset of thermal convection in a saturated porous medium: experiment and analysis

M. KAVIANY

Department of Mechanical Engineering, University of Wisconsin—Milwaukee, Milwaukee, WI 53201, U.S.A.

(*Received* 19 *December* 1983 *and in revised form* 5 *March* 1984)

Abstract—The onset time of convection in a saturated porous medium heated from below is determined analytically and experimentally. By assuming local thermal equilibrium between the fluid and solid phases, linear amplification theory is applied to the governing equations based on local volume averaging. The parameters of the problem are the Rayleigh number, the Prandtl number and the porous medium shape parameter. The dependency of the onset time on these parameters is examined. The onset time is measured for a system composed of glass beads and water. Four different bead diameters are used. In all cases, relatively good agreement is found between the predicted and measured results. The effect of the depth of the medium on the onset time and the validity of the permeability relation used are discussed.

1. INTRODUCTION

THIS study considers the experimental and analytical determination of the onset time of thermal convection in a fluid saturated porous medium subject to transient heating from below. The heating is due to a linear temporal increase in the temperature of the impermeable surface confining the medium from below as shown schematically in Fig. 1. To describe the flow stability in a horizontal layer of a saturated porous medium, the relevant stability analysis technique must be applied to the governing equations for the transport of heat and momentum through two-phase systems. Moreover, in order to treat the system as a continuum, local thermal equilibrium must exist between the phases. These aspects of the analysis are now described briefly.

1.1. *Dynamic stability analysis*

Among the available methods which are suitable for time-dependent temperature fields are: (a) the linear amplification theory [1, 2], (b) the energy method [3], and (c) the nonlinear amplitude method [4]. All lead to the determination of the onset time of convection; and, in the case of the amplitude method, the structure of convection cells in the early stages of their evolution can also be determined. The energy method leads to the lower bound for the time of the onset which is the interval over which the generalized energy of the layer is guaranteed to decay. Of the three techniques, the energy method is the only one that does not need any empirical specification. In the amplification theory the description of the initial conditions and the criterion for marking the time of the onset, in terms of the amplification factor, are made empirically by specifying the required forcing function as found experimentally. However, the time of the onset as predicted by the energy method is about an order of magnitude smaller than that measured in the laboratory [3], while the linear and nonlinear amplification theories [4–6] show better agreement. A detailed discussion of the advantages and disadvantages of the linear amplification theory is given in ref. [2].

1.2. *Local thermal equilibrium*

In describing heat transfer in porous media, the existence of local thermal equilibrium between the fluid and solid phases is required in order to apply local volume averaging. This equilibrium is not always guaranteed [7], especially for time-dependent temperature fields. However, for a given system, a parametric study may be carried out in order to determine whether local thermal equilibrium nearly exists or not. Spiga and Spiga [8] examined the transient response of a fluid–solid system to the variation of temperature imposed on its boundary. They found that for a ramp-type variation in the inlet temperature of a one-dimensional flow with negligible axial conduction, the presence of local thermal equilibrium between the two phases weakly depends on the ratio of the product of the density and specific heat capacity for each phase. However, for transient temperature fields when (a) the axial conduction is not negligible, (b) the thermal conductivities of the solid and fluid phases are different, and (c) the fluid motion is transient and relatively slow (as is the case at the onset of convection), then local thermal equilibrium may not exist.

1.3. *Local volume averaging*

Local volume averaging [9–11] leads to governing equations which, when simplified and combined with the available empirical results [12–14], become readily solvable. These equations include the inertia and boundary effects which are not present in Darcy's equation [15–17].

A full review of the investigation of the onset of convection in porous media, subject to time-independent density distributions, is given by

NOMENCLATURE

a	horizontal wave number [cm^{-1}]	β	coefficient of thermal expansion [K^{-1}]
c	specific heat capacity [$J\ kg^{-1}\ K^{-1}$]	γ	porous medium shape parameter, $(\varepsilon L^2 K^{-1})^{1/2}$
d	diameter of spherical particles [cm]	ε	porosity
g	gravitational constant [$cm\ s^{-2}$]	θ	perturbation component of temperature [K]
$\mathbf{i},\mathbf{j},\mathbf{k}$	unit vectors	μ	dynamic viscosity [$g\ cm^{-1}\ s^{-1}$]
k	thermal conductivity [$W\ m^{-1}\ K^{-1}$]	ν	kinematic viscosity [$cm^2\ s^{-1}$]
K	permeability [cm^2]	ρ	density [$g\ cm^{-3}$]
L	depth of the layer [cm]	ϕ	temporal rate of change of the lower surface temperature [$K\ s^{-1}$].
p	pressure [$N\ m^{-2}$]		
Pr	Prandtl number, $\nu_f \alpha_e^{-1}$	Subscripts	
Ra	Rayleigh number, $g\beta_f \phi L^5 \nu_f^{-1} \alpha_e^{-2} (\rho c)_f \varepsilon (\rho c)_e^{-1}$	c	critical value
		e	effective property, defined for a scalar quantity b as: $b_e = b_f\varepsilon + b_s(1-\varepsilon)$
t	time [s]	f	fluid
T	temperature [K]	i	initial
$\bar{T}$	unperturbed temperature [K]	rms	root mean square
$\mathbf{u}$	velocity vector	s	solid
u, v, w	perturbation components of velocity [$cm\ s^{-1}$]	t, x, y, z	derivatives with respect to t, x, y, z
		0	reference.
$\bar{w}$	defined in equation (12)		
x, y, z	space coordinates [cm].		
Greek symbols			
α	thermal diffusivity [$cm^2\ s^{-1}$]		

Combarnous and Bories [18]. Since then, new investigations have been reported [14, 19–22]. However, with the exception of refs. [14, 21, 22], they either apply the governing equation suggested by Wooding [15], which does not include the boundary effect, or they use equations recommended by Katto and Masouka [23] which are heuristic although they have some similarities to the more formally developed equations. With the exception of recent work by Nield [24], all the other theoretical investigations have dealt with uniform porosity distribution in the medium. In ref. [24] the non-uniformity of the porosity at and near the interface of the medium and the bounding rigid surface was modeled by introducing a plane fluid layer which is bounded by the porous medium and the rigid surface. Then, by applying the proper interfacial boundary conditions [25], Nield found an expression for the critical Rayleigh number for the case of linear temperature profiles. However, this expression contains a constant that must be determined experimentally and its magnitude is not yet available.

In the present study the time of the onset of convection is predicted using the linear amplification theory while assuming that the porosity distribution is uniform and that local thermal equilibrium exists. The onset time is also measured in a medium where glass beads are used as the solid phase with water as the saturating fluid.

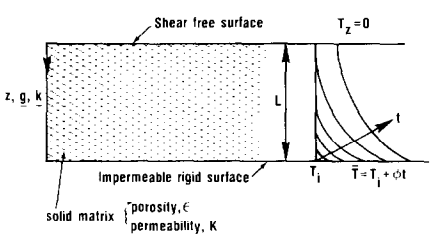

FIG. 1. A schematic of the problem considered.

2. GOVERNING EQUATIONS AND SOLUTION

The governing equations applied are those recommended in refs. [12, 14]. These reduce to their conventional forms for the case involving single-phase media, i.e. when the magnitude of the permeability is infinite. When the local volume averaging symbols are dropped and the Boussinesq approximation is invoked, the linearized forms of the equations are

$$\nabla \cdot \mathbf{u} = 0 \tag{1}$$

$$\rho_f \mathbf{u}_t = -\nabla p - \mu_f \varepsilon K^{-1} \mathbf{u} + (\rho_f)_0 \times [1 + \beta_f (T - T_0)] g\mathbf{k} + \mu_f \nabla^2 \mathbf{u} \tag{2}$$

and

$$(\rho c)_e T_t + (\rho c)_f \varepsilon (\mathbf{u} \cdot \nabla) T = k_e \nabla^2 T. \tag{3}$$

Since there is no mean velocity, the velocity field present is only that due to the perturbation components, i.e.

$$\mathbf{u} = \mathbf{i}u + \mathbf{j}v + \mathbf{k}w \tag{4}$$

where the coordinate system considered is shown in Fig. 1. The temperature field consists of a mean (unperturbed) component $\bar{T}$ and a perturbed component θ, where it is assumed that $\bar{T} = \bar{T}(z, t)$ only.

By combining equations (1)–(3), eliminating the pressure from the momentum equations, and linearizing for infinitesimal perturbations, we have

$$\left(\partial_t - \nu_f \nabla^2 + \frac{\nu_f \varepsilon}{K}\right)\nabla^2 w = -\beta_f g \nabla_1^2 \theta \tag{5}$$

$$\theta_t + (\rho c)_f \varepsilon (\rho c)_e^{-1} w \bar{T}_z = \alpha_e \nabla^2 \theta \tag{6}$$

$$\bar{T}_t = \alpha_e \bar{T}_{zz} \tag{7}$$

where

$$\nabla_1^2 = \partial_{xx} + \partial_{yy}.$$

Equations (5) and (6) describe the dynamic behavior of the perturbation quantities and equation (7) describes the mean temperature field.

The boundary and initial conditions for w, θ and T, which are similar to the conditions present in the laboratory experiment of this study, are:

(i) $$\bar{T}(z, t = 0) = T_i$$
$$\theta(x, y, z, t = 0) = \theta_i$$
$$w(x, y, z, t = 0) = w_i; \tag{8a}$$

(ii) $$\bar{T}(L, t) = T_i + \phi t$$
$$\theta(x, y, L, t) = 0$$
$$w(x, y, L, t) = w_z(x, y, L, t) = 0; \tag{8b}$$

(iii) $$\bar{T}_z(0, t) = 0$$
$$\theta_z(x, y, 0, t) = 0$$
$$w(x, y, 0, t) = w_{zz}(x, y, 0, t) = 0. \tag{8c}$$

Periodic behavior in the horizontal plane is assumed for the perturbation quantities. This horizontal periodicity is characterized by the horizontal wave number, a.

The variables of the problem are now non-dimensionalized using L, $L^2\alpha_e^{-1}$, $\phi L^2 \alpha_e^{-1}$, $\nu_f \alpha_e g^{-1} \beta_f^{-1} L^{-3}$ and $\alpha_e L^{-1}$ to scale the length, time, mean temperature perturbed temperature, and velocity. The non-dimensionalized equations then become

$$[\partial_t + Pr(a^2 - \partial_{zz}) + \gamma^2 Pr](\partial_{zz} - a^2) \times w = a^2 Pr\,\theta \tag{9}$$

$$\theta_t + Ra\, w \bar{T}_z = (\partial_{zz} - a^2)\theta \tag{10}$$

$$\bar{T}_t = \bar{T}_{zz} \tag{11}$$

where γ is the porous medium shape parameter [12]. The solutions to equations (9)–(11) are discussed in refs. [1, 2, 5]. The method of solution for equations (9) and (10) employs the inner Galerkin method [26], which is based on applications of trial functions that satisfy the boundary conditions. Equations (9) and (10) are reduced to initial value ordinary differential equations and are then integrated numerically [5]. As mentioned previously, the amplification theory does not completely describe the physics of the system [2]. However, good agreement is found between the results of this theory and experimental results when the proper initial conditions and the amplification factor for marking the time of the onset are used [1, 2, 5]. Here a 'white noise' initial condition [1] is used and an amplification factor of 1000 is used as the criterion for the time of the onset. This means that the time at which

$$\bar{w} = \left[\int_0^1 w^2(z, t)\,dz \Big/ \int_0^1 w^2(z, t = 0)\,dz\right]^{1/2} \tag{12}$$

reaches a value of 1000 is called the critical time.

As has been shown [1, 2, 5], for a given rate of increase of the lower surface temperature ϕ, the depth of the fluid has no effect on the magnitude of the dimensional onset time when the depth is larger than some critical value. In order to demonstrate the extent of the penetration of the amplified disturbances into the fluid layer, a local perturbation velocity is also defined as

$$w_{rms} = \left[w^2(z, t) \Big/ \int_0^1 w^2(z, t = 0)\,dz\right]^{1/2}. \tag{13}$$

The time of the onset can now be determined as a function of the parameters of the problem, i.e.

$$t_c = t_c(Ra, \gamma^2, Pr, a_c)$$

where a_c is the wave number that results in the shortest critical time. This shortest critical time is called the onset time.

3. EXPERIMENT

A series of experiments were performed and the onset time of convection was measured using glass beads for the solid phase and water as the fluid.

3.1. *Apparatus*

An available [5] test cell was used with inside dimensions of 13 (width) × 7.5 (depth) × 16 (height) cm. The top was covered by an adjustable urethane foam block. The base consisted of a lead block with imbedded copper tubes which together formed a heat exchanger. The fluid running through the copper tubes passed through an adjustable temperature circulator in a closed loop. The test cell rested on a 1.3 × 2.4 m vibration isolation table. Thermocouples were placed in the lead block near the surface and inside the porous medium, both in the beads and in the pores. Their output was monitored and stored at a preselected rate in a digital voltmeter. All the results reported here are for a temporal rate of increase of the lower surface temperature ϕ of approximately 1 K min^{-1}.

3.2. *Porosity and permeability*

Four different diameter glass beads were used with the average diameters and standard deviations (given in parentheses) of 0.3037 (0.0622), 0.3988 (0.0403), 0.5065 (0.0699) and 0.5967 (0.0570), all in centimeters. The

histograms of the beads were similar to those reported by Katto and Masouka [23]. The porosity was determined by randomly packing a known number of beads and measuring the volume of water required to fill the pores. In general, the porosity determined in this manner depended on the number of bead layers and complete reproduction of the results was not always possible. Therefore, for each bead size several porosity measurements were made at each of the several depths considered. The average values for porosity found from these measurements were 0.394, 0.407, 0.393, 0.406 for 0.3, 0.4, 0.5, and 0.6 cm beads, respectively. Since these porosity values were nearly identical, then the average of these values, i.e. $\varepsilon = 0.400$, was used for all bead sizes and depths. The minimum and maximum depths considered were 2.97 and 9.80 cm, respectively. For the spherical beads considered, the following empirical relation [23] was used to determine the permeability

$$K = \frac{\varepsilon^3}{150(1-\varepsilon)^2} d^2. \tag{14}$$

Some of the models [27] resulting in equation (14) are based on flow fields that have a single dominating flow direction. This is not the case at the onset of convection. Therefore, it is interesting to determine whether equation (14) is valid for the problem considered in this study. It should be mentioned that this expression has been used successfully in the experimental determination of marginally stable states for the case of steady-state temperature fields [18, 23].

3.3. *Determination of the onset time*

The actual onset of convection is detected by two methods. The first is by monitoring the temperature at the lower surface of the cell. When convection starts, a readily observable, abrupt change will occur in the rate of heat transfer from the base which can be readily observed. Prior to the onset of convection, the slope of the curve is kept constant (by increasing the temperature of the circulator by given and equal amounts and at given and equal time intervals). At the onset time the slope changes and will have a smaller magnitude while the rate of increasing the circulator temperature is kept the same. The second method is by monitoring the temperature near and above the lower surface. This is done by placing a bead-imbedded thermocouple approximately one bead distance from the lower surface and also placing a thermocouple in the pore volume next to it. At the onset of convection the output of the bead and pore thermocouples will suddenly change as the convection currents begin. A sample of time histories for the base, pore and bead thermocouples is shown in Fig. 2.*

As shown in Fig. 2, due to the particular transient

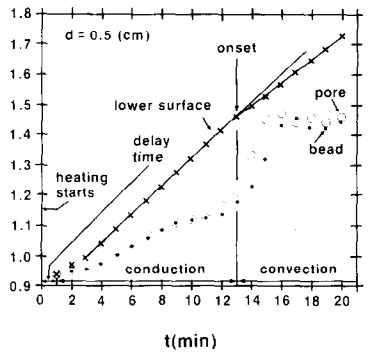

FIG. 2. Temporal variations of the base, bead and pore temperatures. There are about 41 (μV) to 1 (K) in this range of temperature.

response of the heat exchanger to changes made in the circulator temperature, initially the temperature of the lower surface does not increase in the desired linear manner. There is a delay period between the time at which the circulator temperature is first raised and the time at which the temperature in the lower surface of the last cell begins to increase. This period is called the delay time and is marked in Fig. 2. By taking the interception of the linear portion and the initial temperature, a starting time can be obtained. However, the nonlinear portion also makes a contribution. For large onset times, this nonlinear portion will make up only a small portion of the conduction period. Therefore, as the onset time increases this uncertainty becomes less significant.

For the glass bead and water combination and for the temperature range used, the Rayleigh number ranges from 1.41×10^7 to 4.46×10^9 and γ^2 ranges from 8.44×10^3 to 1.84×10^5.

4. PREDICTED RESULTS

The predicted results are given in Figs. 3–9. A Prandtl number of 2.3 which corresponds to a temperature of 50°C (for the water–glass bead system) was chosen. The dependency of the results on the Prandtl number and the temperature at which the thermophysical properties were evaluated are discussed later.

4.1. *Critical wave number*

Figure 3 shows the variation of the critical time with respect to the wave number. The magnitude of the onset time reported hereafter corresponds to the wave number that results in the smallest critical time which is the critical wave number, a_c. In general, as the Rayleigh number and the porous medium parameter, γ, increase, the t_c (a) curve becomes more shallow and a_c increases.

Figure 4 shows the variation of the critical wave number (corresponding to the minimum critical time) with respect to the square of the porous media shape parameter. For this particular set of Ra and Pr, the critical wave number is not significantly dependent on

* Note that up to the time of the onset, a near local thermal equilibrium exists as is demonstrated by the near identical temperatures of the bead and its adjacent pore.

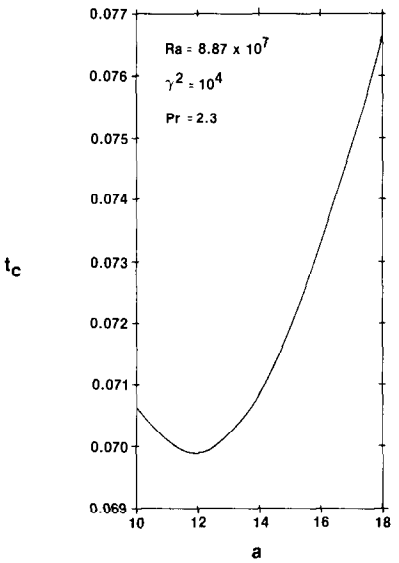

FIG. 3. Variation of the critical time with wave number. The onset time is the minimum point for the critical time. The results are for $Ra = 8.87 \times 10^7$, $\gamma^2 = 10^4$ and $Pr = 2.3$.

γ^2 for $\gamma^2 < 2 \times 10^3$. As the Rayleigh number increases, this limit on γ^2 also increases.

The effects of the physical and dimensionless parameters on the onset time are now discussed.

4.2. *Effect of layer depth*

Figure 5 shows the distributions of the RMS of the perturbation velocity and the mean temperature for a few values of γ^2 at the time of the onset. The results show that as γ^2 increases the effect of heating penetrates further into the layer and the time of the onset increases. For this particular set of Ra and Pr, the effect of heating has reached the top surface for $\gamma^2 = 3 \times 10^4$ as can be seen from the increase in the temperature of the upper surface. However, even for this value of γ^2, the penetration is not significant because the location of the maximum of w_{rms} is still near the lower surface. As will be shown later, this indicates that the dimensional time of the onset is nearly independent of the depth of the layer [1, 2, 5].

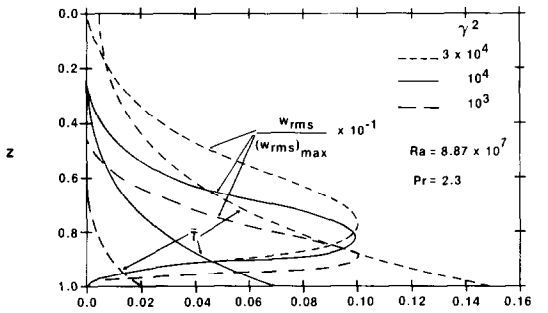

FIG. 5. Distributions of the RMS of the vertical perturbation velocity and the mean temperature for various values of the square of the porous media shape parameter. The results are for $Ra = 8.87 \times 10^7$ and $Pr = 2.3$.

4.3. *Effect of Prandtl number*

Figure 6 shows the effect of the Prandtl number on the onset time for $Ra = 8.87 \times 10^7$. The onset time is normalized with respect to its value for $Pr = 2.3$. The results show that as γ^2 increases the effect of Pr on the onset time decreases.

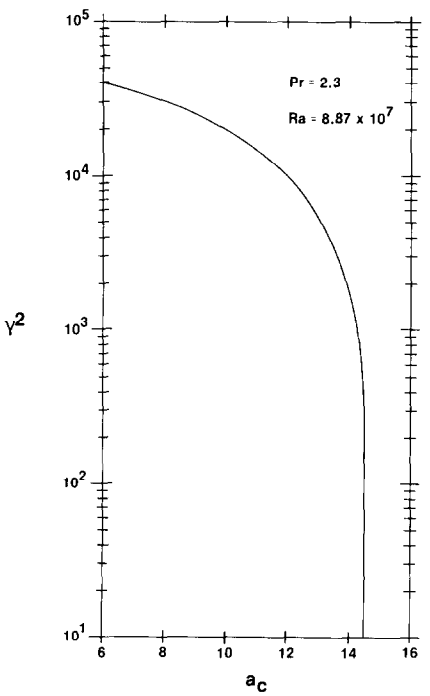

FIG. 4. Variation of the critical wave number with the square of the porous media shape parameter. The results are for $Ra = 8.87 \times 10^7$ and $Pr = 2.3$.

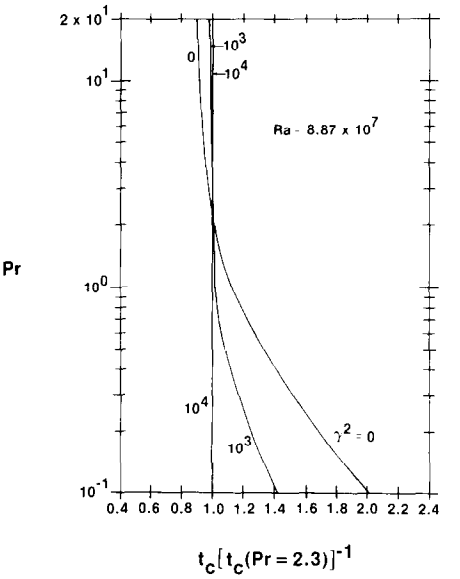

FIG. 6. Variation of the onset time with the Prandtl number for various values of the square of the porous media shape parameter. The results are for $Ra = 8.87 \times 10^7$.

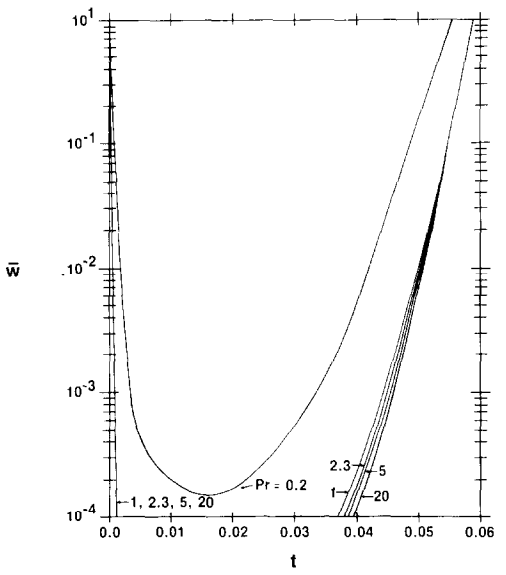

FIG. 7. Decay and growth of the average perturbation velocity with time for various Prandtl numbers. The results are for $Ra = 8.87 \times 10^7$ and $\gamma^2 = 10^3$.

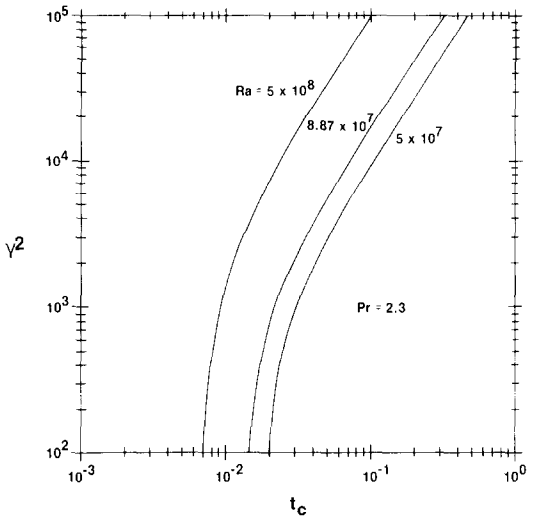

FIG. 8. Variation of the magnitude of the onset time with the square of the porous media shape parameter for various Rayleigh numbers. The results are for $Pr = 2.3$.

This trend can be realized through examination of equation (9). As γ^2 increases, the last term in the square bracket dominates the rest of the terms in the bracket. Meanwhile, the buoyancy term on the RHS is also proportional to the Prandtl number which then results in the relative independency of equation (9) from the Prandtl number. Note that θ is made dimensionless using viscosity. Therefore, by keeping Ra constant (as in Fig. 6), a certain relationship is required between the physical properties of the system. In general, it should be recognized that as Ra increases the onset time becomes less dependent on the Prandtl number, regardless of the value of γ^2.

As was mentioned before, the amplification theory does not completely describe the physics of the system considered here [2]. However, this initial value approach does describe some features of the system. For example, for a given Rayleigh number, as the Prandtl number increases* the onset is delayed. Figure 7 shows this delay and also shows how the magnitude of the average perturbation velocity first decays and then grows. Once the growth begins it proceeds very rapidly and in a super exponential manner. The results for $Pr = 1, 2.3, 5$ and 20 are nearly the same. The results are for $Ra = 8.87 \times 10^7$ and $\gamma^2 = 10^3$.

4.4. *Effect of porous medium shape parameter*

Figure 8 shows the dependency of the onset time on Ra and γ^2 for $Pr = 2.3$. For the three Rayleigh numbers shown, the effect of the solid matrix on the onset time is significant only when $\gamma^2 > 10^3$. The results also show that for a sufficiently large γ^2 (for a given Rayleigh number) the onset time is proportional to γ^2 raised to a power of approximately 1/2, i.e. $t_c = A + B\gamma$ for large γ, where A and B depend on Ra and Pr. Note that γ is the ratio of the large length scale L to the small length scale $K^{1/2}$. Since Ra depends on L and not K, then keeping Ra constant and increasing γ implies a decrease in small length scale. This will be further discussed in presenting the experimental results.

Figure 9 also shows the variation of the onset time with respect to Ra and γ^2 for $Pr = 2.3$. The results are for $Ra \geqslant 10^6$. As has been shown [1, 2, 5], as long as $Ra > 10^6$, for $\gamma^2 = 0$ (layer composed of water only), the dimensional onset time is independent of the fluid layer thickness. Since the Rayleigh number is propor-

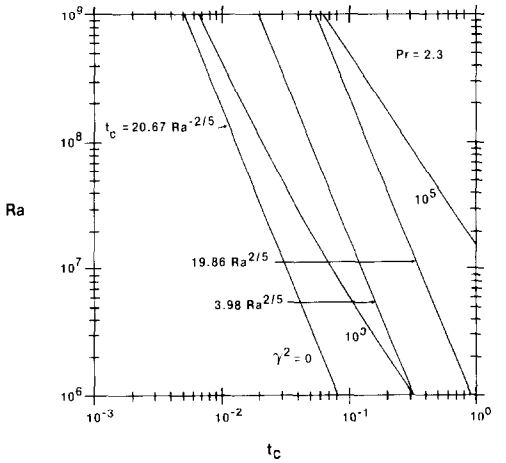

FIG. 9. Variation of the magnitude of the onset time with the Rayleigh number for various values of the square of the porous media shape parameter. The results are for $Pr = 2.3$.

* Note that in order to keep Ra constant, $\nu_f \alpha_e^2$ must remain constant while ν_f increases to increase Pr.

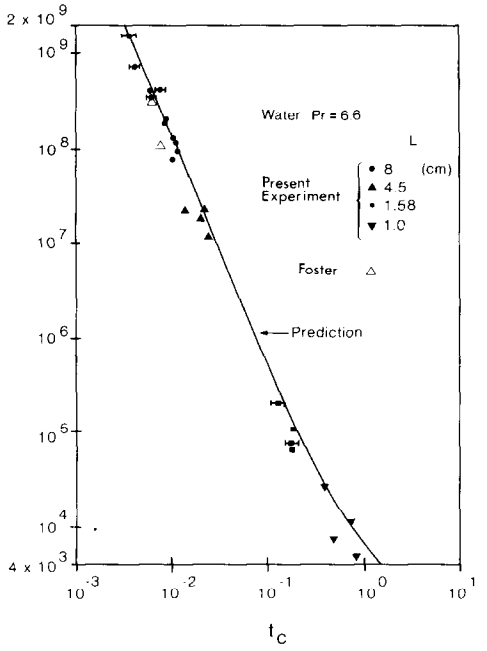

FIG. 10. Variation of the magnitude of the onset time with the Rayleigh number for a layer composed of water only (i.e. $\gamma = 0$).

tional to the fifth power of the layer thickness and the non-dimensionalized time is inversely proportional to the second power of the layer thickness, this independency requires that t_c be proportional to Ra raised to the $-2/5$ power. Due to the presence of the solid matrix ($\gamma^2 \neq 0$), the onset is delayed. Since γ^2 is proportional to the second power of the fluid depth, by increasing γ^2 such that it remains proportional to Ra raised to the 2/5 power, the porosity and permeability of the layer will be kept the same while increasing its depth. Therefore, if the Rayleigh number is large enough, such that the layer thickness does not affect the dimensional onset time, then the onset time will remain proportional to Ra raised to the $-2/5$ power. This is shown for $\gamma^2 = 3.98Ra^{2/5}$ and $\gamma^2 = 19.86Ra^{2/5}$ where the independency of the dimensional onset time from the depth persists.

The results shown in Fig. 9 for $\gamma^2 = 10^3$ and 10^5 show that while for $Ra > 10^8$ the effect of $\gamma^2 = 10^3$ in delaying the onset is not very significant, for $\gamma^2 = 10^5$ this delay is very significant, even for $Ra = 10^9$.

5. EXPERIMENTAL RESULTS AND COMPARISON

Figure 10 shows the variations in the onset time with the Rayleigh number for water alone (i.e. $\gamma^2 = 0$). These previously obtained results [5] show good agreement between the predictions of the linear amplification theory and the experimental results. Also shown are the experimental results of Foster [6].

In comparing the experimental and theoretical results for the onset time, three aspects of the analysis are scrutinized, namely, (a) the validity of the governing equations used and the applicability of linear amplification theory, (b) the validity of the asumption of a uniform porosity distribution, and (c) the applicability of the permeability relation. However, in making the comparison it is not possible to completely isolate the dependency of the onset time from each of these, but as will be shown some conclusions can be made.

For each of the bead sizes, experiments were conducted for various layer thicknesses. Each experiment was repeated several times to insure reproducibility. Table 1 gives the results for beads of diameter 0.3 cm. The physical properties of water were evaluated at the surface temperature at the onset time. This was done in order to account for the concentration of buoyancy force near the heated surface. Both the dynamic viscosity and the volumetric thermal expansion coefficients depend rather strongly on the temperature. The properties of the beads were taken to be those of window glass [29] with a density, specific heat capacity and thermal conductivity of 2700 kg m^{-3}, 840 J kg^{-1} K^{-1}, and 0.78 W m^{-1} K^{-1}, respectively. The intention was to keep the value of ϕ at 1 K min^{-1}, but small deviations were inevitable. In presenting the experimental results, for each experimental condition the onset time is given in a range rather than as a single value, because of the uncertainty in interpreting the experimental results (Fig. 2).

The results given in Table 1 show that the measured dimensional onset time is independent of the layer thickness. The dimensional onset time for a plane water

Table 1. Comparison between the measured onset times, $t_{c,m}$, and predicted onset times, $t_{c,p}$, for the glass beads of $d = 0.3$ cm in water

L (cm)	ε	α_e (m^2 s^{-1})	β_f (K^{-1})	Pr	ϕ (K min^{-1})	γ^2	Ra	$t_{c,m}$ (min)	$t_{c,m}$	$t_{c,p}$	Error (%)
2.97	0.4	2.37×10^{-7}	381×10^{-6}	2.79	1.04	3.31×10^4	2.20×10^7	17.6–19.5	0.28–0.31	0.36	22.2–13.9
3.64					1.13	4.97×10^4	6.61×10^7	18.0–20.0	0.19–0.21	0.24	20.8–12.5
4.20					1.10	6.62×10^4	1.32×10^8	17.5–19.4	0.14–0.16	0.18	22.0–13.8
4.97					1.18	9.26×10^4	3.28×10^8	17.5–19.4	0.10–0.11	0.13	23.1–14.7
5.42					1.21	1.10×10^5	5.18×10^8	17.6–19.4	0.085–0.094	0.107	20.6–12.4
5.92					1.18	1.31×10^5	7.82×10^8	17.5–19.6	0.071–0.080	0.092	22.8–13.6
6.80					1.10	1.73×10^5	1.54×10^9	17.7–19.6	0.055–0.061	0.069	20.3–11.7

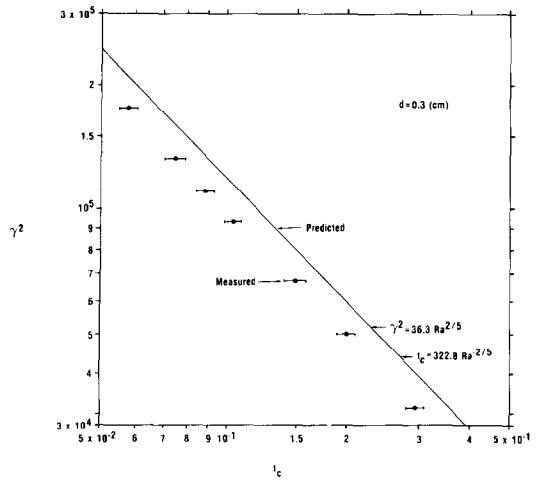

FIG. 11. Variation of the magnitude of the onset time with the square of the porous media shape parameter. The predicted results are for $Pr = 2.3$ and the experimental results are for $d = 0.3$ cm.

layer, i.e. $\gamma = 0$, is 1.63 min, which indicates that the onset time for this particular case has increased approximately twelvefold. Of course, as the diameter of the beads increases, this delaying effect is reduced and vice versa.

The results given in Table 1 show that the measured onset times are between 12–23% (3–5 min) lower than the predicted values. Similar results are found for the 0.4, 0.5, and 0.6 cm diameter beads. The percentages of error, for all cases, were between 12–28%. Moreover, the measured onset times were lower than the predicted values. Since the results for the other bead diameters are approximately the same as those for $d = 0.3$ cm, they are not reported here. The measured onset time was lower than the predicted values for all bead diameters. Possible causes of this deviation will be discussed later.

The results given in Table 1 are also shown in Fig. 11. The predicted relationships between t_c, Ra and γ, which indicate the independence of the dimensional onset time from the layer thickness, are also given.

As previously mentioned, when Ra is kept constant the predicted results show that for a relatively large γ, the variation in t_c can be approximated as $t_c = A + B\gamma$. When L is also kept constant, then an increase in γ corresponds to a decrease in the small length scale. The small length scale is the bead diameter for the case of spherical particles since K is proportional to d^2 and $\gamma^2 = \varepsilon L^2 K^{-1}$. Therefore, it is expected that the dimensional onset time varies nearly in proportion to d^{-1}. In order to observe this relationship a Rayleigh number of 5×10^8 was chosen and experiments were performed for this particular value.

Table 2 shows the experimental and predicted results for this Rayleigh number. The layer thickness for different bead diameters had to be slightly different in order to compensate for the changes in the thermophysical properties. Examination of the results indicates that the increase in the dimensional onset time corresponding to decreases in the bead diameter is as expected, i.e. t_c is nearly proportional to d^{-1}.

The results given in Table 2 are also shown in Fig. 12. An approximate linear relationship between t_c and γ for $Ra = 5 \times 10^8$ and $\gamma^2 > 7 \times 10^4$ is also shown. The relatively good agreement that exists between the measured and predicted results indicates that the permeability relation used, i.e. K proportional to d^2, is appropriate for the transient flow field associated with the onset of convection.

A number of non-ideal features of the experimental system have not been included in the analysis. For example, (a) the porosity non-uniformity at and near the rigid surface, (b) horizontal anisotropy in the structures of the solid matrix or in the temperature of the heated surface, (c) the deviation of the mean temperature field from one-dimensionality (due to the presence of the side walls), and (d) temperature dependency of viscosity. These, in general, accelerate the onset of convection. Furthermore, since the buoyancy force is concentrated near the rigid boundary, the non-uniformity in porosity can play an even more significant role than was found by Nield [24] for linear temperature profiles. However, such an effect must depend on the particle size, i.e. in Nield's model the thickness of the plane fluid layer depends on the particle size. But in the experimental results obtained here, a particle size dependency cannot be readily recognized (Fig. 12). Therefore, although the relatively high porosity at and near the heated surface does cause acceleration of the onset, its effect cannot be readily rationalized.

The differences between the experimental and predicted results should be considered as acceptable. Furthermore, in the absence of experimental results using other porous media, such as fibers, no dominant

Table 2. Comparison of the measured onset times, $t_{c,m}$, and predicted onset times, $t_{c,p}$, for several different glass bead diameters and Rayleigh number of 5×10^8

d (cm)	L (cm)	ϕ (K min^{-1})	ε	α_e (m^2 s^{-1})	Pr	β_f (K^{-1})	γ^2	Ra	$t_{c,m}$ (min)	$t_{c,m}$	$t_{c,p}$	Error (%)
0.3	5.41	1.20	0.4	2.37×10^{-7}	2.79	381×10^{-6}	1.1×10^5	5×10^8	17.5–19.4	0.085–0.094	0.107	20.6–12.4
0.4	5.64	1.19			3.08	341×10^{-6}	6.7×10^4		12.6–15.0	0.056–0.067	0.078	28.2–14.1
0.5	5.77	1.18			3.24	320×10^{-6}	4.5×10^4		10.3–12.0	0.044–0.051	0.060	26.7–15.0
0.6	5.84	1.18			3.32	310×10^{-6}	3.2×10^4		8.85–10.0	0.037–0.042	0.048	22.9–12.5

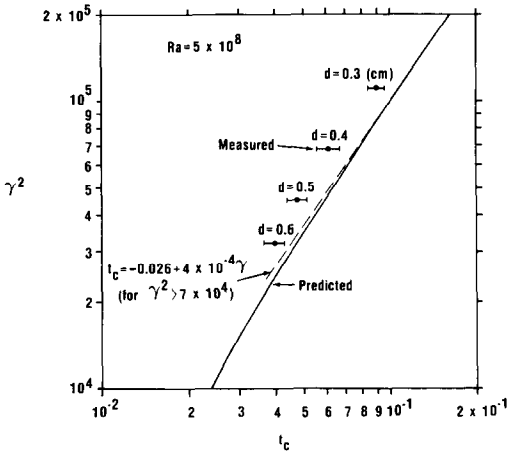

FIG. 12. Variation of the magnitude of the onset time with the square of the porous media shape parameter. The predicted results are for $Pr = 2.3$ and $Ra = 5 \times 10^8$. Also shown is an approximation made to predicted results.

cause for the discrepancy can be identified, but the partial list given above can be among the contributors.

6. SUMMARY

The time of the onset of convection in a horizontal layer of saturated porous media subject to transient heating from below is predicted by the linear amplification theory and is measured using media composed of glass beads and water. The time of the onset depends on the Rayleigh number, Ra, the porous media shape parameter, γ, and the Prandtl number, Pr.

The predicted results, based on the assumption of local thermal equilibrium and uniform porosity distribution, show that

(a) For $Ra > 10^6$ the delay in the onset of convection, caused by the presence of the solid matrix, is significant only for $\gamma^2 > 10^3$.

(b) For $Ra > 10^6$ and $\gamma^2 > 10^4$, the onset time is independent of the Prandtl number.

(c) For a given Ra and for relatively large γ^2, the onset time is inversely proportional to the square root of permeability.

Relatively good agreement is found between the predicted and measured results. The experimental results show that

(a) Up to the time of the onset of convection, near local thermal equilibrium exists between the glass beads and water filled pores.

(b) The applied expression relating the permeability to particle diameter is valid for the transient flow field associated with the onset of thermal convection.

Acknowledgement—The support of the National Science Foundation, through Grant MEA 82-04837, is appreciated.

REFERENCES

1. T. D. Foster, Stability of a homogeneous fluid cooled uniformly from above, *Physics Fluids* **8,** 1249–1257 (1965).
2. E. G. Mahler, R. S. Schechter and E. H. Wissler, Stability of a fluid layer with time-dependent density gradients, *Physics Fluids* **11,** 1901–1912 (1968).
3. P. C. Wankat and G. M. Homsy, Lower bounds for the onset of instability in heated layers, *Physics Fluids* **20,** 1200–1201 (1977).
4. G. Ahlers, M. C. Cross, P. C. Hohenberg and S. Safran, The amplitude equation near the convective threshold: application to time-dependent heating experiments, *J. Fluid Mech.* **110,** 297–334 (1981).
5. M. Kaviany, Onset of thermal convection in a fluid layer subjected to transient heating from below, *Trans. Am. Soc. Mech. Engrs*, Series C, *J. Heat Transfer*, in press.
6. T. D. Foster, Onset of manifest convection in a layer of fluid with time-dependent surface temperature, *Physics Fluids* **12,** 2482–2487 (1969).
7. Y. T. Chan and S. Banerjee, Analysis of transient three-dimensional natural convection in porous media, *Trans. Am. Soc. Mech. Engrs*, Series C, *J. Heat Transfer* **103,** 242–248 (1981).
8. G. Spiga and M. Spiga, A rigorous solution to a heat transfer two-phase model in porous media and packed beds, *Int. J. Heat Mass Transfer* **24,** 355–364 (1981).
9. J. C. Slattery, Two-phase flow through porous media, *A.I.Ch.E. Jl* **16,** 345–352 (1970).
10. S. Whitaker, Advances in theory of fluid motion in porous media, *Ind. Engng Chem.* **61,** 14–28 (1969).
11. P. Cheng, Heat transfer in geothermal systems, *Adv. Heat Transfer* **14,** 1–105 (1978).
12. K. Vafai and C. L. Tien, Boundary and inertia effects on flow and heat transfer in porous media, *Int. J. Heat Mass Transfer* **24,** 195–203 (1981).
13. K. Vafai and C. L. Tien, Boundary and inertia effects on convective mass transfer in porous media, *Int. J. Heat Mass Transfer* **25,** 1183–1190 (1982).
14. P. C. Wankat and W. R. Schowalter, Stability of combined heat and mass transfer in porous medium, *Physics Fluids* **13,** 2418–2420 (1970).
15. R. A. Wooding, Steady state free thermal convection of liquid in a saturated permeable medium, *Physics Fluids* **12,** 273–285 (1957).
16. F. A. Kulacki and R. Ramchandani, Hydrodynamic instability in a porous layer saturated with a heat generation fluid, *Wärme- und Stoffübertragung* **8,** 179–185 (1975).
17. D. A. Nield, Onset of thermohaline convection in a porous medium, *Wat. Resour. Res.* **4,** 553–560 (1968).
18. M. A. Combarnous and S. A. Bories, Hydrothermal convection in saturated porous media, *Adv. Hydrosci.* **10,** 231–307 (1975).
19. G. M. Homsy and A. E. Sherwood, Convective instabilities in porous media with through flow, *A.I.Ch.E. Jl* **22,** 168–174 (1976).
20. K. Walker and G. M. Homsy, A note on convective instabilities in Boussinesq fluids and porous media, *Trans. Am. Soc. Mech. Engrs*, Series C, *J. Heat Transfer* **99,** 338–339 (1977).
21. N. Rudraiah, B. Verrappa and S. Balachandra Rao, Convection in a fluid-saturated porous layer with non-uniform temperature gradient, *Int. J. Heat Mass Transfer* **25,** 1147–1156 (1982).
22. M. Kaviany, Thermal convective instabilities in porous medium, *Trans. Am. Soc. Mech. Engrs*, Series C, *J. Heat Transfer* **106,** 137–142 (1984).
23. Y. Katto and T. Masouka, Criterion for the onset of convective flow in a fluid in a porous medium, *Int. J. Heat Mass Transfer* **10,** 297–309 (1967).
24. D. A. Nield, The boundary correction for the Rayleigh–

Darcy problem: limitation of the Brinkman equation, *J. Fluid Mech.* **128,** 37–46 (1983).
25. G. S. Beavers and D. D. Joseph, Boundary conditions at a naturally permeable wall, *J. Fluid Mech.* **30,** 197–207 (1967).
26. L. J. Snyder, T. W. Spriggs and W. E. Stewart, Solution of the equation of change by Galerkin's method, *A.I.Ch.E. Jl* **10,** 535–540 (1964).
27. F. A. L. Dullien, *Porous Media, Fluid Transport and Pore Structure*, p. 159. Academic Press, New York (1979).
28. A. E. Scheidegger, *The Physics of Flow Through Porous Media*, p. 150. University of Toronto Press, Toronto (1974).
29. J. P. Holman, *Heat Transfer* (5th edn.), p. 538. McGraw Hill, New York (1981).

APPARITION DE LA CONVECTION THERMIQUE DANS UN MILIEU SATURE: EXPERIENCE ET ANALYSE

Résumé—Le temps d'apparition de la convection dans un milieu poreux saturé chauffé à sa base est déterminé analytiquement et expérimentalement. En supposant un équilibre thermique local entre le fluide et le solide, la théorie d'amplification linéaire est appliquée aux équations basées sur la moyenne locale en volume. Les paramètres du problème sont le nombre de Rayleigh, le nombre de Prandtl et le paramètre de forme du milieu poreux. La dépendance du temps d'apparition vis-à-vis de ces paramètres est examinée. Le temps d'apparition est mesuré pour un système composé de billes de verre et d'eau. On utilise quatre diamètres de billes. Dans tous les cas, on trouve un accord relativement bon entre les résultats des mesures et les calculs. On discute l'effet de la profondeur du milieu sur le temps d'apparition et la validité de la relation de perméabilité utilisée.

DAS EINSETZEN DER KONVEKTION IN EINER ÜBERFLUTETEN SCHÜTTUNG; EINE EXPERIMENTELLE UND THEORETISCHE UNTERSUCHUNG

Zusammenfassung—Die Zeit bis zum Einsetzen der Konvektion in einer überfluteten, von unten beheizten Schüttung wird analytisch und experimentell bestimmt. Unter Annahme eines örtlichen thermischen Gleichgewichts zwischen flüssiger und fester Phase wird die Theorie der linearen Verstärkung auf die Bestimmungsgleichungen angewandt, wobei örtliche Mittelwerte zugrundegelegt werden. Die Parameter sind die Rayleigh-Zahl, die Prandtl-Zahl und der Formfaktor der Schüttung. Der Einfluß dieser Parameter auf die Zeit bis zum Einsetzen der Konvektion wird untersucht. Die Zeit bis zum Einsetzen der Konvektion wird an einer Anordnung aus Glasperlen und Wasser gemessen. Vier verschiedene Durchmesser wurden verwendet, und in allen Fällen wurde recht gute Übereinstimmung zwischen berechneten und gemessenen Ergebnissen festgestellt. Der Einfluß der Tiefe der Schüttung auf die Zeit bis zum Einsetzen der Konvektion und die Gültigkeit der verwendeten Permeabilitätsbeziehung werden diskutiert.

ВОЗНИКНОВЕНИЕ КОНВЕКТИВНОГО ТЕПЛОПЕРЕНОСА В НАСЫЩЕННОЙ ПОРИСТОЙ СРЕДЕ: ЭКСПЕРИМЕНТ И АНАЛИЗ

Аннотация—Аналитически и экспериментально определено время возникновения конвективного теплопереноса в нагреваемой снизу насыщенной пористой среде. Основные уравнения, полученные при усреднении локального объема, решаются в предположении локального теплового равновесия между жидкой и твердой фазами. Параметрами задачи являются числа Рэлея и Прандтля, а также параметр, определяющий форму пористой среды. Исследована зависимость времени возникновения конвективного переноса от этих параметров. Время возникновения конвекции измеряется для системы, состоящей из стеклянных шариков и воды. Используются шарики четырех различных диаметров. Во всех случаях найдено довольно хорошее совпадение результатов расчета с измеренными значениями. Обсуждается влияние глубины среды на время возникновения конвекции и на справедливость используемого выражения для проницаемости среды.